Monotonic, Cyclic, and Post-cyclic Behaviour of Fine Gravel

Mathan V. Manmatharajan, MASc, P.Eng.
PhD Candidate & Senior Geotechnical Engineer
Department of Civil and Mineral Engineering, University of Toronto, Toronto, &
WSP Golder, Mississauga, ON

Alex Sy, PhD, P.Eng.
Vice President, Technical
Klohn Crippen Berger, Vancouver, BC

Mason Ghafghazi, PhD, P.Eng.
Assistant Professor
Department of Civil and Mineral Engineering, University of Toronto, Toronto, ON.

ABSTRACT
Historically, gravelly soils had often been considered to be less susceptible to liquefaction because of their coarser particles and higher permeability. However, the liquefaction of gravelly soils has been observed across the world since 1891 to recent earthquakes (1891 Mino-Owari, Japan; 1983 Borah Peak, USA; and 2014 Cephalonia, Greece). Behaviour of gravelly soils during earthquakes is not as well understood as that of sands even though case-histories have revealed that gravelly soils are susceptible to liquefaction. Laboratory studies conducted using triaxial tests on gravelly soils reported that particle gradation and size have a profound influence on behaviour of gravelly soils despite the issue of membrane compliance. A comprehensive laboratory investigation of gravelly soils could provide valuable insights into gravelly soil behaviour.

The behaviour of a natural fine gravel is studied through a critical state soil mechanics framework. Drained triaxial compression tests were used to determine critical state line and its parameters. A large, 30.7 cm diameter cyclic simple shear device was used to understand the cyclic response and post-cyclic response of this fine gravel. Both relative density and state parameter were used to quantify the liquefaction resistance and post-liquefaction strength. The liquefaction resistance of the fine gravel did not appear to be stronger than that of clean sands, but the post-liquefaction strength of the fine gravel appeared to be stronger than that of clean sand at the same state.

RÉSUMÉ
Historiquement, les sols graveleux ont souvent été considérés comme moins sensibles à la liquéfaction en raison de leurs particules plus grossières et de leur perméabilité plus élevée. Cependant, la liquéfaction des sols graveleux a été observée dans le monde entier depuis 1891 jusqu'à des séismes récents (1891 Mino-Owari, Japon ; 1983 Borah Peak, USA ; et 2014 Cephalonia, Grèce). Le comportement des sols graveleux pendant les tremblements de terre n'est pas aussi bien compris que celui des sables, même si des études de cas ont révélé que les sols graveleux sont susceptibles de se liquéfier. Des études de laboratoire réalisées à l'aide d'essais triaxiaux sur des sols graveleux ont montré que la gradation et la taille des particules ont une profonde influence sur le comportement des sols graveleux, malgré la question de la conformité de la membrane. Une étude complète en laboratoire des sols graveleux pourrait fournir des informations précieuses sur le comportement des sols graveleux.

Le comportement d'un gravier fin naturel est étudié dans le cadre de la mécanique des sols à l'état critique. Des essais de compression triaxiale drainée ont été utilisés pour déterminer la ligne d'état critique et ses paramètres. Un grand dispositif de cisaillement simple cyclique de 30,7 cm de diamètre a été utilisé pour comprendre la réponse cyclique et post-cyclique de ce gravier fin. La densité relative et les paramètres d'état ont été utilisés pour quantifier la résistance à la liquéfaction et la résistance post-liquéfaction. La résistance à la liquéfaction du gravier fin ne semblait pas être plus forte que celle des sables propres, mais la résistance post-liquéfaction du gravier fin semblait être plus forte que celle du sable propre au même état.

1 INTRODUCTION

Earthquakes are among the deadliest natural disasters causing extensive damage to communities across the world. A significant portion of the damage caused by earthquakes is caused by soil liquefaction. The term liquefaction refers to the significant loss of strength and stiffness resulting from the generation of excess pore water pressure in saturated soils due to seismic and sometimes static loading. Liquefaction occurs in soils with a wide range of particles, such as silts, sands and gravels, and their mixtures, when ground shaking causes a tendency of

densification. Liquefaction of gravelly soils, even though less frequent than that of sands, has been observed since 1891 to recent earthquakes: (e.g., 1891 Mino-Owari, Japan; 1908 San Francisco, USA; 1964 Alaska, USA; 1983 Borah Peak, USA; 1988 Armenia; 1995 Kobe, Japan; 2008 Wenchuan, China; 2014 Cephalonia, Greece; and 2016 Kaikoura, New Zealand). Even though case-histories (e.g., Ishihara 1985; Youd et al. 1985; Harder and Seed 1986; Nikolaou et al. 2015; and Cubrinovski et al. 2019) have revealed that gravelly soils are susceptible to liquefaction, they have often been considered to be less susceptible to liquefaction because of their coarser particles and higher permeability. However, the permeability of clean uniform gravel needs to be differentiated from that of gravelly soils where gravel, sand and silt-sized particles within the matrix control permeability. The behaviour of gravelly soils during and following earthquake loading is not as well understood as that of sands. Thus, understanding the behaviour of gravelly soils and the mechanisms involved in the liquefaction of gravelly soils is imperative. A comprehensive laboratory investigation of gravelly soils could provide valuable insights into gravelly soil behaviour.

Several researchers (e.g., Holts and Gibbs 1956; Lee and Fitton 1969; Wong et al. 1974; Chang and Ko 1982; Evans and Zhou 1995; Kokusho et al. 2004; Hubler 2017; and Xu et al. 2019) have investigated liquefaction susceptibility of gravelly soils using laboratory testing. Performing laboratory tests on gravelly soils is always challenging because of their particle size demanding larger equipment and specimens. With the exception of Hubler (2017) and Xu et al. (2019), all researchers used triaxial tests. Membrane compliance plays a significant role in determining liquefaction resistance in triaxial testing, especially under undrained conditions. Evans et al. (1992) reported that liquefaction resistance could be under- or overestimated by the membrane compliance effect that in turn increases as particle size increases.

Gradation has a first-order effect on the dilative and contractive behaviour of soils. For example, Holts and Gibbs (1956) and Evans and Zhou (1995) stated that shear strength increases as gravel content increases (sand content decreases) up to 50-60% in the gravel-sand composite mixtures at a given relative density. Monotonic shear strength has been reported to be higher for well-graded soils than that of uniformly graded soils (e.g. Kokusho et al. 2004; and Flora et al. 2012). Studies by Kokusho et al. (2004) and Hubler (2017) revealed that liquefaction resistance was not influenced by gradation and particle size in triaxial and simple shear conditions, respectively.

Residual shear strength of liquefied soil is another important parameter controlling deformation during earthquake loading. Many researchers have studied the shear strength of liquefied sand in laboratory using both triaxial and simple shear apparatuses (e.g., Ishihara et al. 1990; Vaid and Thomas 1995; Olson and Stark 2003; and Sivathayalan and Mehrabi Yazdi 2013). Laboratory studies have indicated that shear strength of liquefied soils depends on relative density (or state parameter) at the end of consolidation, loading mode (triaxial compression, extension, simple shear), consolidation stress, and the maximum shear strain at the initial liquefaction.

A few researchers (e.g., Kokusho et al. 2004; Hubler 2017; and Xu et al. 2019) have studied the post-cyclic behaviour of gravelly soils in laboratory. Xu et al. (2019) reported that post-cyclic monotonic shear strength of simple shear specimens consolidated to 200 kPa vertical effective stress and 36% relative density was slightly increased with the inclusion of gravel content up to 40%. Kokusho et al. (2004) reported that sandy gravel exhibits almost 10 times higher post-liquefaction strength than sand at 20% axial strain and concluded that post-liquefaction undrained strength at large strains (~20%) mostly depends on gradation and particle size in triaxial. Hubler (2017) concluded that post-cyclic shear strength increases with increasing particle size in simple shear as well.

This paper aims at understanding the behaviour of a uniform fine gravel as part of a comprehensive study focusing on effect of gradation and particle size on liquefaction triggering of granular soils. The behaviour of a natural fine uniformly graded gravel is studied using the state parameter as well as relative density. Drained triaxial compression tests were used to determine critical state properties. A large, 30.7 cm diameter, cyclic simple shear device was used to quantify the liquefaction resistance and post-cyclic behaviour of the gravel. The results were compared to well-known materials.

2 MATERIAL AND TESTING

2.1 Material

The gravel studied was from Hutcheson quarry in Huntsville, Ontario, Canada. The quarry is located on a glaciolacustrine deposit and was selected due to its relative proximity to the research laboratory while originating from the Canadian Shield, thus containing more common minerals (quartz and feldspar) than soils that are found in Toronto. Fine Hutcheson gravel (FHG) was separated from the bulk samples received. The particle size distribution of FHG is shown in Figure 1 along with its material properties. The FHG has sub-rounded to rounded particles (Sphericity, S = 0.77, Roundness, R = 0.65) and consists of 31% of quartz, 30% of potassium feldspar, 15% of amphibole, 15% of plagioclase feldspar, 6% of biotite, and 3% other minerals.

2.2 Testing Equipment

Two testing devices; triaxial and simple shear were used in this study and discussed in the following sections.

2.2.1 Triaxial

A series of drained triaxial compression tests were conducted on fine gravel to determine its critical state properties. A 13 kN load cell was used and the specimen was sheared by controlling displacement through a microprocessor-controlled drive unit. A volume change device with a capacity of 100 ml was used to measure the volume of water going in or out of the specimen. A Linear Variable Differential Transformer (LVDT) with a maximum stroke of 25 mm was used to measure the axial displacement. Cell and back pressures were applied by a

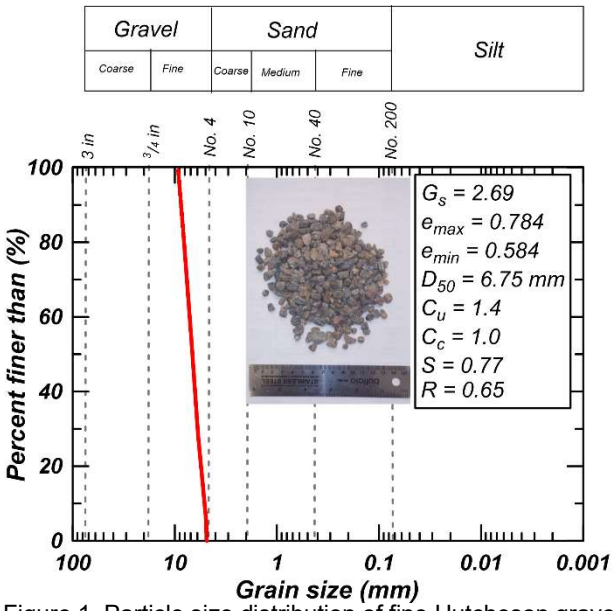

Figure 1. Particle size distribution of fine Hutcheson gravel (FHG) *S: Sphericity, R: Roundness*

pressure control panel. Specimens had a diameter of 100 mm and a height of 200 mm and were reconstituted using air pluviation. Drained tests were preferred to eliminate a need for membrane penetration correction. A fixed top cap was used to avoid excessive tilting of the top cap at high strains (Mozaffari et al. 2022).

Upon completion of sample preparation, CO_2 and deaired water were flushed through the sample one after another to achieve a "B" value of 0.96 or higher as a confirmation for a high degree of saturation. The specimen was then isotopically consolidated to a desired confining stress and sheared using displacement-controlled loading at a rate of 5% axial strain per hour. Details of the triaxial apparatus used in this study are further described in Manmatharajan (2022).

2.2.2 Large cyclic simple shear

A Royal Swedish Geotechnical Institute (SGI) type large cyclic simple shear apparatus (LCSS) manufactured by Geocomp was used for this study at the University of Toronto. Figure 2 shows the LCSS device which accommodates a cylindrical specimen with a diameter of 307 mm and height of ~105 mm. A series of 6.35 mm thick Teflon-coated stacked rings were used to enable K_0 conditions and maintain constant diameter during monotonic and cyclic loading. A latex membrane was used between the specimen and the inner radius of the stacked rings to protect the stacked rings and prevent loss of particles. The LCSS consists of grooved top and bottom platens to establish good friction with particles. The device permits maximum consolidation stress of 600 kPa and cyclic shear stress of 300 kPa controlled by stepper and servo motors, respectively. The vertical and horizontal movement are measured using potentiometers with a range of 100 mm stroke and 0.001 mm resolution. Further details of the LCSS device are described in Manmatharajan (2022).

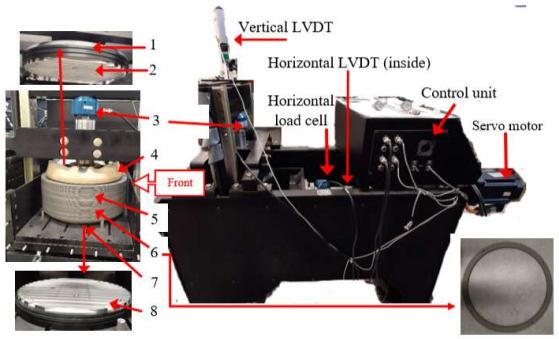

1.Top cap	2. Top grooved porous stone	3.Vertical load cell	4. Membrane
5. Specimen	6. Teflon stacked rings	7. Bottom pedestal	8. Bottom grooved porous stone

Figure 2. Large cyclic simple shear device at University of Toronto

2.3 Triaxial tests

Figure 3 shows the results of the triaxial tests. As can be seen in Figure 3, the specimen was sheared to reach 20% or higher axial strain. When gradation was checked before and after each test, particle breakage was observed on specimens consolidated to 200 kPa vertical effective stress or more. Particle breakage was assessed and corrected using the framework proposed by Ghafghazi et al. (2014). This framework determines the end point of a test had particle breakage not occurred, by correlating the change in gradation to the shift in the critical state line.

Figures 3a and 3c show volumetric response and shear stress ratio of FHG against axial strain, respectively. Figures 3b and 3d show void ratio and deviator stress change against mean effective stress, respectively. In Figure 3b, open symbols represent data from original tests (before particle breakage correction) and closed symbols represent the results after particle breakage correction. The critical state line shown in Figure 3b (red-solid line) was determined after particle breakage correction. The critical state parameters, Γ (intercept at p'_{cs}=1 kPa) = 1.040, λ_{10} (slope of the CSL) = 0.130, and M_{tc} (ratio of q and p') = 1.56, ϕ_{cs} (critical state friction angle) = 38.2°.

Figure 4 presents the relation between maximum dilatancy $(D = -\varepsilon_v/\varepsilon_q)$ and the state parameter at maximum dilatancy. It also compares the fine gravel (FHG) with a large database of generally uniformly graded clean sands and tailings compiled by Jefferies and Been (2015). The data from FHG fall nicely within the database from literature. FHG fits χ_{tc} of 3, which is very close to 3.5 taken as a typical value for clean sands (Jefferies 1993).

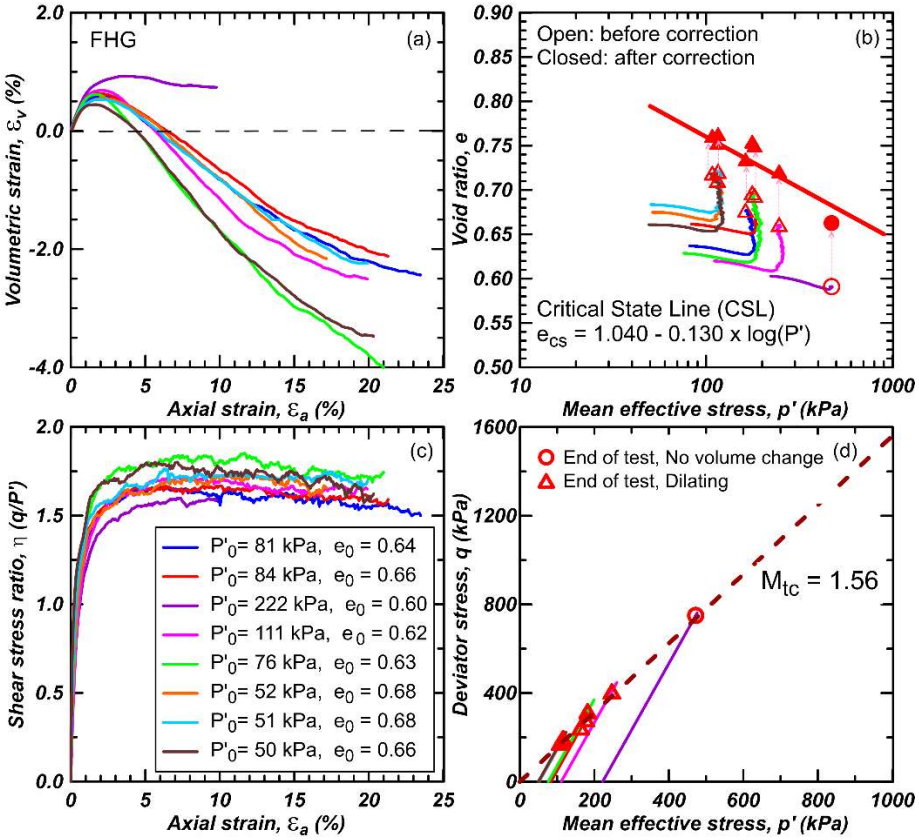

Figure 3. Drained triaxial compression tests for FHG: (a) volumetric strain versus axial strain (b) void ratio versus mean effective stress (c) stress ratio versus axial strain (d) deviator stress versus mean effective stress

2.4 LCSS tests

Twenty-two cyclic tests were conducted on FHG specimens consolidated 50 and 100 kPa vertical effective stress over a range of void ratios (loose to dense) as shown in Table 1. All these tests were followed by post-cyclic monotonic shearing to at least 25% shear strain. Specimens, 307 mm in diameter and 105 mm in height, were air-pluviated, in which, a weight of about 13 kg dry fine gravel was poured through a funnel with about 25 mm spout diameter from about a 5 mm drop height. To make the loosest possible specimens (D_{r0} < 20%), the funnel was kept at center and raised slowly to maintain constant drop height. For medium to dense specimen, the funnel was moved around in a circular pattern at a constant drop height. Very dense specimens (D_{r0} > 80%) were prepared by tapping on the preparation table. Details of specimen preparation are available in Manmatharajan (2022). To establish contact between the top cap and the gravel, two cycles of loading to 3.25 mm displacement were applied under 3 kPa vertical stress. The displacement amplitude was determined as half of the median grain size (D_{50}) of the gravel, to hypothetically ensure particles were not rolled and only slightly adjusted at the contact. The specimen was then consolidated to desired vertical effective stresses (σ'_{vc}) of 50 or 100 kPa. At the end of consolidation, the void ratio (e_0) was determined using the dry weight and the known cell volume.

Following consolidation, cyclic tests were sheared under constant volume conditions at a rate of 0.1 Hz. Initial liquefaction was defined when the single amplitude shear strain reached ±3.75%. Figure 5 depicts an example of cyclic test results and post-cyclic test results (5f and 5g) of a specimen consolidated to 100 kPa vertical effective stress and 49% relative density. Initial liquefaction was observed at 13 uniform cycles.

Figure 6 shows Cyclic Stress Ratio (CSR) plotted against the number of cycles to cause initial liquefaction at 100 kPa vertical effective stress. This Figure helps estimate the Cyclic Resistance Ratio (CRR) at 15 uniform cycles for various relative densities (and state parameters). As can be seen, CRR increases as relative density increases at 15 uniform cycles.

Figure 7 shows the variation of Cyclic Resistance Ratio (CRR), which was determined at 15 cycles, with state parameter and relative density at post-consolidation for 50 kPa and 100 kPa vertical effective stress. The CRR increases with decreasing state parameter value and increasing relative density for both vertical effective stresses. Vertical effective stresses (50 and 100 kPa) show no significant difference in CRR. For Figure 7a, the state parameter was calculated using the CSL inferred from the drained triaxial compression tests as described in section 2.3. The mean effective stresses (p') required to get the state parameter was calculated using the coefficient of lateral earth pressure at rest, K_0 which was assumed to be 0.5.

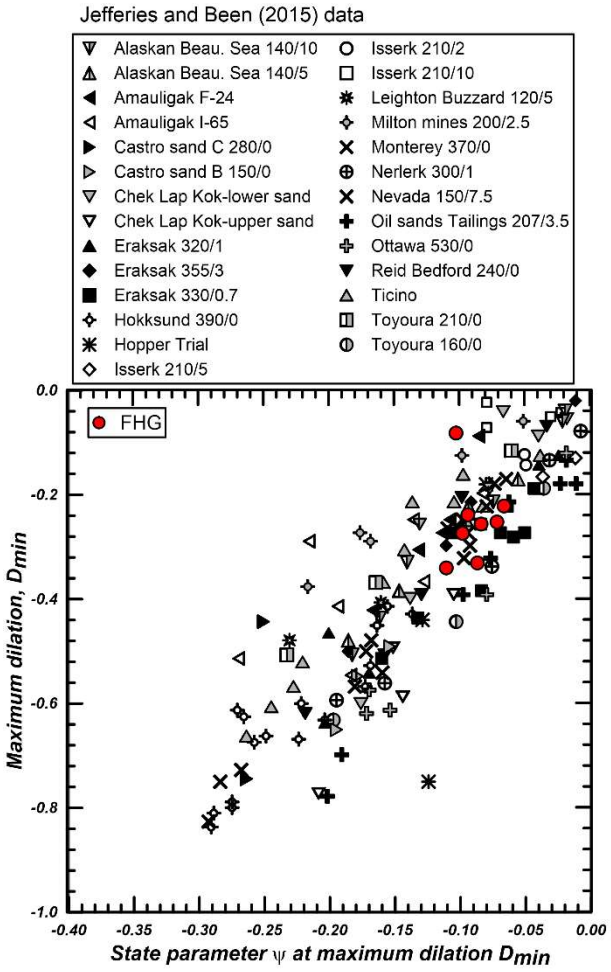

Figure 4. Minimum dilatancy versus the state parameter for both natural soils and tailings from Jefferies and Been (2015) database and fine gravel (FHS)

Table 1. Summary of cyclic tests in large simple shear

σ'_{vc} (kPa)	e_0	D_{r0} (%)	ψ_0	CSR	# of tests
50	0.785 - 0.636	0 - 75	-0.057 to -0.206	0.09 0.10	11
100	0.799 - 0.647	8 - 82	-0.003 to -0.156	0.11 0.12	11

σ'_{vc}- Vertical effective stress at the end of the consolidation
e_0 – Void ratio at the end of the consolidation
D_{r0} – Relative density at the end of the consolidation
ψ_0 – State parameter at the end of the consolidation

Figure 7 compares the results obtained from this study (FHG), Fraser River sand (FRS) and Ottawa sand (OS), which suggest little or no major effect of particle size. Triaxial test result on moist tamped specimens were used to determine critical state lines by Ghafghazi (2011) and Murthy (2006) for FRS and OS, respectively. Cyclic simple shear test results were obtained from Sivathayalan (1994) and Manmatharajan (2011) for FRS and OS, respectively. In cyclic testing, Sivathayalan (1994) used water pluviated specimens while Manmatharajan (2011) used air pluviated specimens. Figure 7 shows the CRRs of FRS and OS are slightly higher than those of FHG with both state parameter and relative density as reference. However, the difference is small towards the loose end and overall, not significant given that all data occupy a narrow range of CRRs. Similar observation was made by Kokusho et al. (2004) and Hubler (2017). Vertical effective stresses appear to have no influence on the CRRs in both state parameter and relative density approach.

Post-cyclic monotonic shearing was performed immediately at the end of the cycle when initial liquefaction (±3.75% shear strain) occurred. Figure 5f depicts shear stress-shear stress response and 5g depicts the stress path of both cyclic and post-cyclic monotonic response. All specimens showed strain hardening post-liquefaction. This is simply explained given that at low effective stresses occurring at initial liquefaction, the specimen is well below the critical state line, resulting in strong dilation upon monotonic shearing. Figure 8 shows a summary of the post-cyclic (residual) strengths (S_r), at 5%, 10%, and 20% shear strains plotted against state parameter obtained at the end of consolidation (ψ_0), relative density (D_{r0}), and post-cyclic state parameter (ψ_{cy}). Relative density would be the same for both as all the tests is constant volume. As can be seen, S_r increases with decreasing ψ_0 value, increasing D_{r0} and decreasing ψ_{cy} at all three strain levels.

Figure 9 compares the residual strength ratio (residual stress normalized by post-consolidation vertical stress) of FHG at 20% shear strain and recommended residual strength curves from Idriss and Boulanger (2008). For FHG, equivalent clean sand CPT normalized corrected tip resistance ($q_{c1Ncs-Sr}$) was determined using post-consolidation relative density and equation [1] recommended by Idriss and Boulanger (2008).

$$D_R = 0.478\, {q_{c1N}}^{0.264} - 1.063 \qquad [1]$$

The CPT resistance is conceptual in this case to connect the residual strengths obtained to field measurements. Otherwise, CPT testing is not practical in gravels. The FHG results appeared to be higher than the trend lines reported by Idriss and Boulanger (2008) but not far from their case history data. The literature data were largely from sandy sites with FHG having more than five times higher particle size (D_{50}). This suggests that particle size influences the residual strength as also observed by Kokusho et al. (2004) and Hubler (2017).

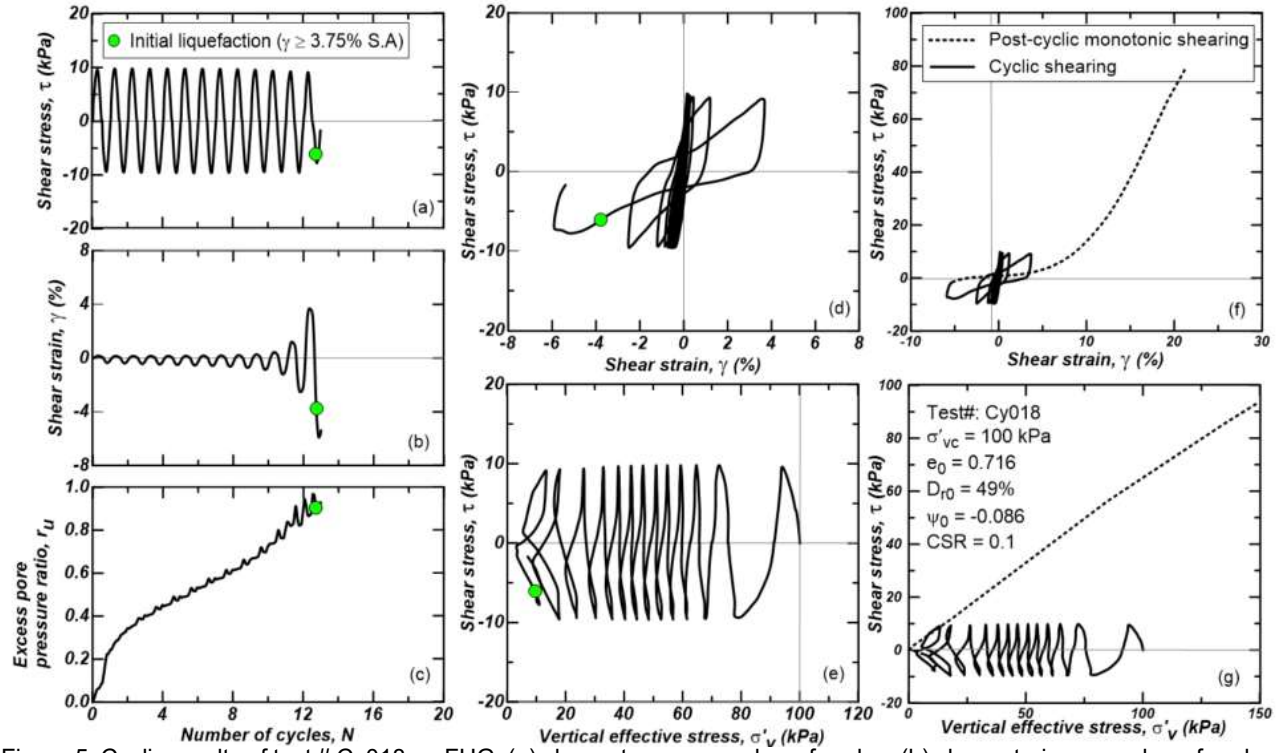

Figure 5. Cyclic results of test # Cy018 on FHG: (a) shear stress vs number of cycles, (b) shear strain vs number of cycles, (c) excess pore pressure vs number of cycles, (d) shear stress-shear strain response, (e) stress path, (f) shear stress-shear strain response of cyclic and post cyclic shearing, (g) shear stress-shear strain response of cyclic and post-cyclic shearing at σ'_{vc} =100 kPa, D_{r0}= 49%, ψ_0=-0.086

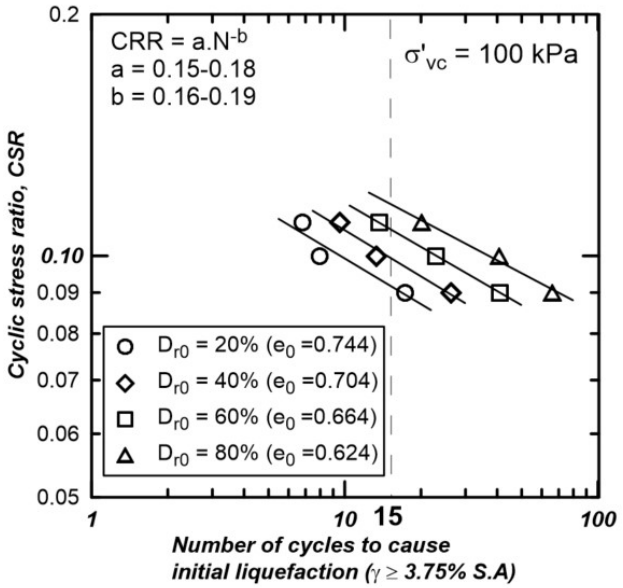

Figure 6. Comparison of CSR and number of cycles to cause initial liquefaction at 100 kPa

3 SUMMARY AND CONCLUSIONS

A uniform fine gravel (FHG) was tested in a series of drained triaxial compression tests to determine the critical state parameters, and a series of cyclic and post-cyclic monotonic simple shear tests to determine its cyclic resistance and post-cyclic monotonic strength. The results were assessed using both relative density and state parameter and compared to databases from the literature.

The larger particle size of FHG appeared not to influence its dilatancy compared to other sand dominated uniform materials. Fine gravel expresses an increasing trend of cyclic resistance with increasing density in a similar way to clean sands and shows a similar cyclic resistance to well-known clean sands. When viewed in light of their density and confining stress, there is not a clear difference between uniformly graded clean sands and fine gravel. Apart from differences in permeability, there is no mechanical reason why these materials should be different. The gravel showed strain hardening response in post-cyclic monotonic shearing and its residual strength increased with increasing shear strain. Residual strength did appear to be influenced by particle size as observed by the limited existing data on liquefaction of gravelly soils.

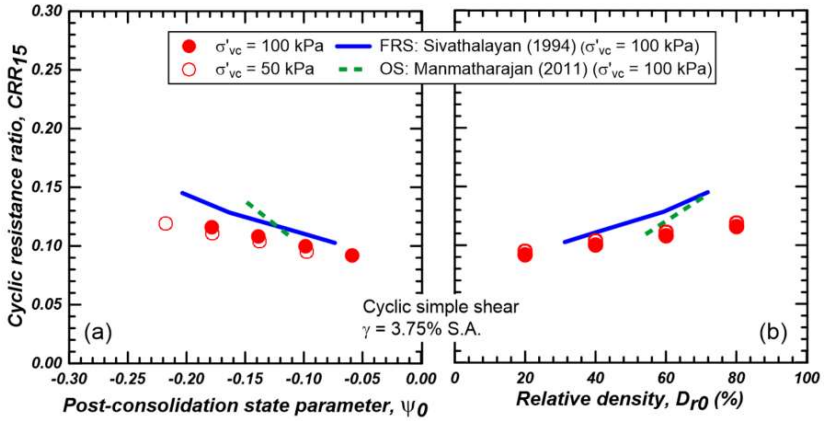

Figure 7. Variation of CRR with (a) state parameter and (b) relative density for all four soils at 50 and 100 kPa

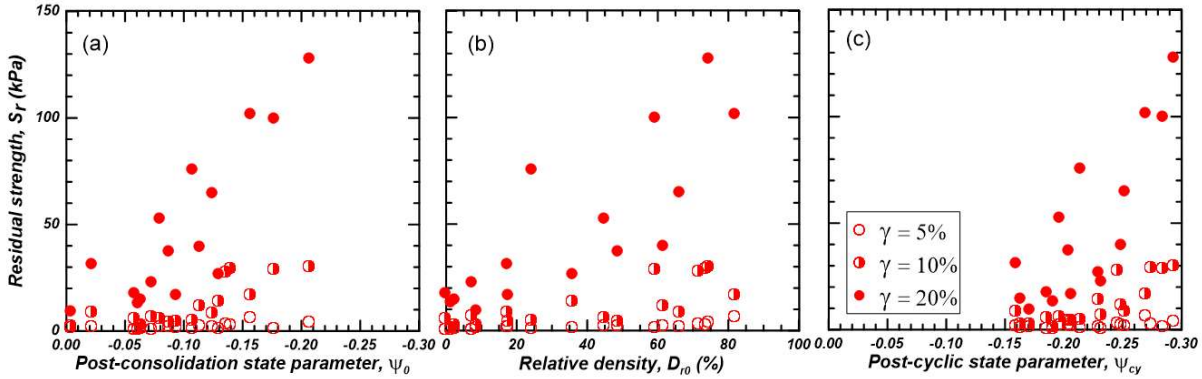

Figure 8. Comparison of S_r against relative density (D_{r0}), state parameter obtained at the end of consolidation (ψ_0), and post-cyclic stat parameter (ψ_{cy}) at 5%, 10%, and 20% shear strain

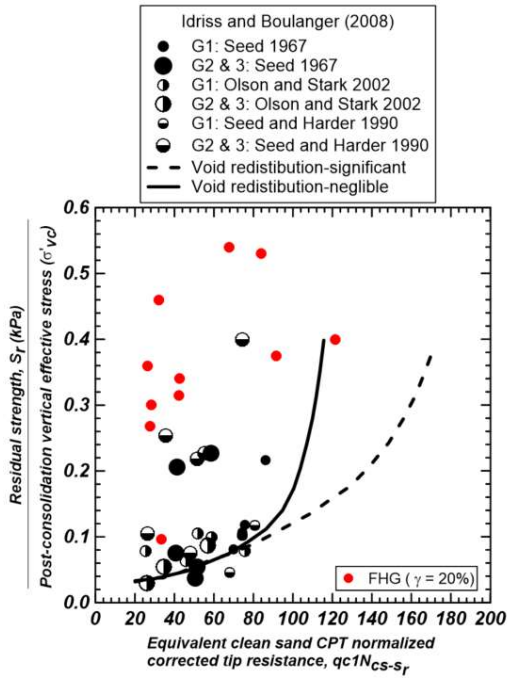

Figure 9. Comparison of S_r against equivalent clean sand CPT normalized corrected tip resistance $q_{c1Ncs-Sr}$

4 ACKNOWLEDGEMENTS

First author has been supported by Natural Science and Engineering Research Council of Canada (Funding reference no. 518439/2018). The authors greatly appreciate the financial support of Klohn Crippen Berger and the Natural Science and Engineering Research Council of Canada (NSERC) (RGPIN-2016-05622).

5 REFERENCES

Cubrinovski, M. Ntritsos, N. Dhakal, R. and Rhodes, A. 2019. Key aspects in the engineering assessment of soil liquefaction.pdf. *In Earthquake Geotechnical Engineering for protection and Development of Environment and Construction*. Edited by S.& Moraci. 2019 Assoziazione Geotechnica Italiana, Rome, Italy.

Evans, M.D. Seed, H.B. and Seed, R.B. 1992. Membrane compliance and liquefaction of sluiced gravel specimens. *Journal of Geotechnical Engineering*, 118(6): 856–872. doi:10.1061/(ASCE)0733-9410(1992)118:6(856).

Evans, M.D. and Zhou, S. 1995. Liquefaction behavior of sand-gravel composites. *Journal of Geotechnical Engineering,* 121(3): 287–298. doi:0733-9410/95/0003-0287-0.298.

Flora, A. Lirer, S. and Silvestri, F. 2012. Undrained cyclic resistance of undisturbed gravelly soils. *Soil Dynamics and Earthquake Engineering*, 43: 366–379. Elsevier. doi:10.1016/j.soildyn.2012.08.003.

Ghafghazi, M. Shuttle, D.A. and DeJong, J.T. 2014. Particle breakage and the critical state of sand. *Soils and Foundation*. 54 (3), 451–461.

Ghafghazi, M. 2011. Towards comprehensive interpretation of the state parameter from Cone Penetration Testing on cohesionless soils. Department of Civil Engineering, The University of British Columbia, Vancouver, Canada.

Murthy, T.G. 2006. Study of the undrained static response of sandy soils in the critical state framework. doi:10.1145/1198467.1198470.

Harder, L.F. and Seed, H.B. 1986. Determination of penetration resistance for coarse-grained soils using the Becker hammer drill. *Report No. UCB/EERC-86/06*, College of Engineering, University of California, Berkeley, California.

Hubler, J.F. 2017. Laboratory and In-Situ Assessment of Liquefaction of Gravelly Soils. PhD Thesis, Depratment of Civil Engineering, The University of Michigan, Michigan, USA.

Idriss, I.M. and Boulanger, R.W. 2008. Soil liquefaction During Earthquakes. *In Earthquake Engineering Research Institute. Earthquake Engineering Research Institute*, Oakland, CA, USA. Available from http://www.eeri.org.

Ishihara, K. 1985. Stability of Natural Deposits during Earthquakes. *In International Society for Soil Mechanics and Geotechnical Engineering (ISSMGE)*. pp. 536–537. doi:10.1007/978-3-319-73568-9_174.

Ishihara, K. 1993. Liquefaction and flow failure during earthquakes. *Géotechnique*, 43(3): 351–451. doi:10.1680/geot.1993.43.3.351.

Ishihara, K. Yasuda, S. and Yoshida, Y. 1990. Liquefaction-induced flow failure of embankments and residual strength of silty sands. *Soils and Foundations*, 30(3): 69–80.

Jefferies M.G. 1993. Nor-sand: a Simple Critical State Model for Sand. *Géotechniqu*e, 43(1): 91-103.

Jefferies, M. and Been, K. 2015. Soil liquefaction: A critical state approach (2nd ed.) *CRC Press*.

Kokusho, T. Hara, T. and Hiraoka, R. 2004. Undrained shear strength of granular soils with different particle gradations. *Journal of Geotechnical and Geoenvironmental Engineering*, 130(6): 621–629. doi:10.1061/(ASCE)1090-0241(2004)130:6(621).

Lee, K.L. and Fitton, J.A. 1969. Vibration Effects of Earthquakes on Soils and Foundations. In Vibration Effects of Earthquakes on *Soils and Foundations*. American Society for Testing and Materials, San Francisco, California. pp71–95. doi:10.1520/stp450.

Manmatharajan, V. 2011. Initial stress state and stress history effects on liquefaction susceptibility of sands. Carleton University.

Manmatharajan, V. 2022. Factors affecting liquefaction assessment of granular soils through laboratory testing. University of Toronto. Toronto, ON. (under final defense).

Mozaffari, M. Liu, W. and Ghafghazi, M. 2022. Influence of Specimen Non-uniformity and End Restraint Conditions on Drained Triaxial Compression Test Results in Sand. Canadian Geotechnical Journal. https://doi.org/10.1139/cgj-2021-0505.

Nikolaou, S. Zekkos, D. Assimaki, D. and Gilsanz, R. 2015. Earthquake Reconnaissance January 26th/February 2nd 2014 Cephalonia, Greece events, Version 1. *In International Society for Soil Mechanics and Geotechnical Engineering (ISSMGE)*.

Olson, S.M. and Stark, T.D. 2003. Use of laboratory data to confirm yield and liquefied strength ratio concepts. *Canadian Geotechnical Journal*, 40(6): 1164–1184. doi:10.1139/t03-058.

Sivathayalan, S. 1994. Static, cyclic and post liquefaction simple shear sesponse of sands. Department of Civil Engineering, The University of British Columbia, Vancouver, Canada.

Sivathayalan, S. and Mehrabi Yazdi, A. 2013. Influence of strain history on postliquefaction deformation characteristics of sands. *Journal of Geotechnical and Geoenvironmental Engineering*, 140(3): 1–14. doi:10.1061/(ASCE)GT.1943-5606.0001037.

Thevanayagam, S. 1998. Effects of fines and confining stress on undrained shear stregth of silty sands. *Journal of Geotechnical and Geoenvironmental Engineering*, 124(June): 479–491.

Vaid, Y.P. and Sivathayalan, S. 2000. Fundamental factors affecting liquefaction susceptibility of sands. *Canadian Geotechnical Journal,* 37(3): 592–606. doi:10.1139/t00-040.

Vaid, Y.P. and Thomas, J. 1995. Liquefaction and postliquefaction behavior of sand. *Journal of Geotechnical Engineering,* 121(2): 163–173. doi:10.1061/(ASCE)0733-9410(1995)121:2(163).

Wong, R.T. Seed, H.B. and Chan, C.K. 1974. Liquefaction of gravelly soils. Earthquake Engineering Research Center, College of Engineering, University of California. Berkeley, California.

Xu, D. sheng, Liu, H.B. Rui, R. and Gao, Y. 2019. Cyclic and postcyclic simple shear behavior of binary sand-gravel mixtures with various gravel contents. *Soil Dynamics and Earthquake Engineering,* 123(March): 230–241. Elsevier Ltd. doi:10.1016/j.soildyn.2019.04.030.

Youd, T.L. Harp, E.L. Keefer, D.K. and Wilson, R.C. 1985. The Borah Peak , Idaho earthquake of Oct . 28 , 1983. Liquefaction, *Earthquake spectra*, 2(1)(December): 71–89.